

Monolithic epitaxy and optoelectronic properties of single-crystalline γ-In_2Se_3 thin films on mica

Xibo Yin(尹锡波), Yifan Shen(沈逸凡), Chaofan Xu(徐超凡), Jing He(贺靖), Junye Li(李俊烨), Haining Ji(姬海宁), Jianwei Wang(王建伟), Handong Li(李含冬), Xiaohong Zhu(朱小红), Xiaobin Niu(牛晓滨), and Zhiming Wang(王志明)

Citation: Chin. Phys. B, 2021, 30 (**1**): 017701. DOI: 10.1088/1674-1056/abcf32
Journal homepage: http://cpb.iphy.ac.cn; http://iopscience.iop.org/cpb

What follows is a list of articles you may be interested in

Thickness-dependent excitonic properties of atomically thin 2H-$MoTe_2$

Jin-Huan Li(李金焕), Dan Bing(邴单), Zhang-Ting Wu(吴章婷), Guo-Qing Wu(吴国庆), Jing Bai(白静), Ru-Xia Du(杜如霞), Zheng-Qing Qi(祁正青)
Chin. Phys. B, 2020, 29 (**1**): 017802. DOI: 10.1088/1674-1056/ab5a3a

Spectral properties of Pr:CNGG crystals grown by micro-pulling-down method

Yan-Yan Xue(薛艳艳), Na Li(李纳), Dong-Hua Hu(胡冬华), Qing-Song Song(宋青松), Xiao-Dong Xu(徐晓东), Dong-Hai Wang(王东海), Qing-Guo Wang(王庆国), Dong-Zhen Li(李东振), Zhan-Shan Wang(王占山), Jun Xu(徐军)
Chin. Phys. B, 2019, 28 (**8**): 087801. DOI: 10.1088/1674-1056/28/8/087801

Influence of annealing treatment on the luminescent properties of Ta:β-Ga_2O_3 single crystal

Xiaowei Yu(余小威), Huiayuan Cui(崔慧源), Maodong Zhu(朱茂东), Zhilin Xia(夏志林), Qinglin Sai(赛青林)
Chin. Phys. B, 2019, 28 (**7**): 077801. DOI: 10.1088/1674-1056/28/7/077801

Enhanced magneto-electric effect in manganite tricolor superlattice with artificially broken symmetry

Huanyu Pei(裴环宇), Shujin Guo(郭蜀晋), Hong Yan(闫虹), Changle Chen(陈长乐), Bingcheng Luo(罗炳成), Kexin Jin(金克新)
Chin. Phys. B, 2018, 27 (**9**): 097701. DOI: 10.1088/1674-1056/27/9/097701

First-principles study of polarization and piezoelectricity behavior in tetragonal $PbTiO_3$-based superlattices

Zhenye Zhu(朱振业)
Chin. Phys. B, 2018, 27 (**2**): 027701. DOI: 10.1088/1674-1056/27/2/027701

Monolithic epitaxy and optoelectronic properties of single-crystalline γ-In_2Se_3 thin films on mica*

Xibo Yin(尹锡波)[1], Yifan Shen(沈逸凡)[2], Chaofan Xu(徐超凡)[1], Jing He(贺靖)[1], Junye Li(李俊烨)[1], Haining Ji(姬海宁)[1], Jianwei Wang(王建伟)[1], Handong Li(李含冬)[1,†], Xiaohong Zhu(朱小红)[2], Xiaobin Niu(牛晓滨)[1,‡], and Zhiming Wang(王志明)[3]

[1] *School of Materials and Energy, University of Electronic Science and Technology of China, Chengdu* 611731, *China*
[2] *College of Materials Science and Engineering, Sichuan University, Chengdu* 610064, *China*
[3] *Institute of Fundamental and Frontier Sciences, University of Electronic Science and Technology of China, Chengdu* 610054, *China*

(Received 7 May 2020; revised manuscript received 7 October 2020; accepted manuscript online 1 December 2020)

The growth of γ-In_2Se_3 thin films on mica by molecular beam epitaxy is studied. Single-crystalline γ-In_2Se_3 is achieved at a relatively low growth temperature. An ultrathin β-In_2Se_3 buffer layer is observed to nucleate and grow through a process of self-organization at initial deposition, which facilitates subsequent monolithic epitaxy of single-crystalline γ-In_2Se_3 at low temperature. Strong room-temperature photoluminescence and moderate optoelectronic response are observed in the achieved γ-In_2Se_3 thin films.

Keywords: γ-In_2Se_3, molecular beam epitaxy, optoelectronic response

PACS: 77.55.Px, 78.55.−m, 85.60.Bt **DOI:** 10.1088/1674-1056/abcf32

1. Introduction

In_2Se_3 can be considered as one of the complex III–VI compounds due to its existence in several allotropic phases, such as α-In_2Se_3 with layered phase,[1] β-In_2Se_3 with rhombohedral phase,[2] γ-In_2Se_3 with defect-wurtzite structure,[3,4] and κ-phase with anisotropic structure.[5] One can find advanced applications of In_2Se_3 of different crystal structures in diverse fields, such as phase-change storage,[6] photovoltaics,[7] optoelectronics,[8] ionic battery,[9] thermoelectrics,[10] and ferroelectronics.[11,12] Among the well-known phases of In_2Se_3, the defect-wurtzite γ-In_2Se_3 exhibits large optical rotary power with a wide band gap ($\sim$ 2 eV), so that it holds great promise for developing novel photonic and optoelectronic devices operated at high temperature.[13,14] For device application purpose, the thin film plays a vital role; thus, there have been many methods employed to obtain γ-In_2Se_3 thin films. γ-In_2Se_3 thin films prepared by magnetron sputtering, source co-evaporation, chemical bath deposition, solid-phase reaction, electrodeposition, and sol-gel technologies are polycrystalline (PC) with inferior electronic and optical quality.[15–17] So far, the single-crystalline (SC) γ-In_2Se_3 films are only obtained by metal-organic chemical vapor deposition (MOCVD) or molecular beam epitaxy (MBE) method. However, the MOCVD growth of γ-In_2Se_3 has to be operated at a temperature higher than 700 K,[18,19] which is incompatible with the microelectronic process required for integrating γ-In_2Se_3 on patterned circuits. As to the MBE approach, Ohtsuka *et al.* obtained SC γ-In_2Se_3 at the growth temperature higher than 573 K and the VI/III ratio between 5 and 15, using GaAs(111)B as substrate.[20] The γ-In_2Se_3 films were proposed to be grown by the so-called van der Waals epitaxy,[20] but their crystallinity was very poor.

Despite all these efforts, the challenge remains to achieve pure phase γ-In_2Se_3 thin films of decent material quality, due to the low phase transition (PT) barriers between In_2Se_3 allotropies. In this study, we manage to integrate SC γ-In_2Se_3 on mica by MBE, as an approach to achieve monolithic SC γ-In_2Se_3 thin films at more accessible growth temperature with decent material quality. It is observed that the initial condensation of In_2Se_3 thin layer undergoes a rapid self-organization process through which an ultrathin β-In_2Se_3 layer is formed on mica surface at low growth temperature (450 K–500 K). The obtained ultrathin layered β-In_2Se_3 then serves as an effective buffer layer and facilitates the subsequent phase-pinned epitaxial growth of γ-In_2Se_3 at conditions far from thermodynamic equilibrium. The as-grown metastable γ-In_2Se_3 thin films exhibit excellent structural stability, crystallinity, and optoelectronic properties, thus are promising for optoelectronics and photonics applications.

*Project supported by the National Key R&D Program of China (Grant Nos. 2018YFA0306102 and 2018YFA0306703), the National Natural Science Foundation of China (Grant No. 61474014), the Sichuan Science and Technology Program, China (Grant No.2019YJ0202), and the University Program for Elaborate Courses of Postgraduates.

†Corresponding author. E-mail: hdli@uestc.edu.cn
‡Corresponding author. E-mail: xbniu@uestc.edu.cn

© 2021 Chinese Physical Society and IOP Publishing Ltd

2. Experimental procedures

The growth of In_2Se_3 thin films was carried out in a customized MBE chamber with a base pressure of $\sim 3 \times 10^{-10}$ mbar. Fluorophlogopite mica chips with 500 μm thick Mo film coated on the back side were used as substrates. A pair of thermocouples were mounted near the sample for monitoring the growth temperature. High purity In (99.9999%) was evaporated from a standard Knudsen cell and Se (99.999%) from a crack cell, respectively. The beam equivalent pressure (BEP) of In and Se was measured by a beam flux monitor (BFM), and In flux was further calibrated by a quartz oscillation crystal (QCO) for precise surface coverage analysis. During the deposition, the Se/In beam equivalent pressure ratio was fixed at 20:1 to create a Se-rich environment.[21,23] At In BEP of $\sim 1 \times 10^{-7}$ mbar, which corresponds to a QCO rate of ~ 2 monolayers (MLs) In on γ-In_2Se_3 (0 0 1) surface per minute, a growth rate of ~ 1 nm (approximately a half unit cell length in c-axis of γ-In_2Se_3) per minute of γ-In_2Se_3 film was achieved as further evidenced by *ex situ* thickness inspection by a profilometer. Noting that one unit cell of γ-In_2Se_3 consists of 4 MLs In along c-axis, we thereby deduced thorough surface incorporation of In adatoms during epitaxial growth of γ-In_2Se_3.

The surface structure evolution of In_2Se_3 during deposition was *in situ* monitored by reflection high energy electron diffraction (RHEED, model RHD-30, SPCES GmbH). The techniques employed to evaluate the quality of obtained γ-In_2Se_3 films include: high-resolution x-ray diffraction (HRXRD, model Bede D1, Jordan Valley), scanning electron microscope (SEM, model InspectF, FEI), energy dispersive x-ray spectrometer (EDS, model INCA, OXFORD), atomic force microscopy (AFM, Veeco), Raman spectroscopy, and photoluminescence spectroscopy (PL, model inVia Raman Microscope, Renishaw). The optoelectronic response of the film was measured under the illumination of a class AAA solar simulator. All measurements were carried out at room temperature.

3. Results and discussion

Upon initiation of In_2Se_3 deposition at 500 K, we observed the RHEED pattern changing abruptly from that of mica to a completely diffusive background (not shown here), indicating a full coverage of amorphous In-Se compound. The subsequent self-organized crystallization of β-In_2Se_3 from the amorphous state occurs at In nominal coverage of ~ 2 MLs (nearly equivalent to one quintuple layer full coverage of layered-In_2Se_3 on the substrate), followed by simultaneous coalescence of single crystalized β-In_2Se_3 adsorbates into big two-dimensional islands on the mica substrate. This is seen by precise in-plane lattice parameter measurement by the RHEED, i.e., the value D as defined in Fig. 1(a) as well as by the coexisting streaky 1×1 surface reconstructed patterns of mica and β-In_2Se_3 shown in Fig. 1(b). As the In coverage increases from ~ 2 MLs to ~ 6 MLs, the RHEED pattern changes gradually from that of β-In_2Se_3 to the characteristics of γ-In_2Se_3 (see Fig. 1(c)), and the observed $\sqrt{3} \times \sqrt{3}$ pattern exactly reflects the In-vacancy honeycomb sublattice structure of γ-In_2Se_3 in *c*-plane (Fig. 1(d)). It suggests a competitive growth process of the In_2Se_3 film, during which the emerged γ-In_2Se_3 phases eventually surpass the metastable β-In_2Se_3 phases as thickness increases (denoted by $\beta \rightarrow \gamma$ process hereafter). The metastable β-In_2Se_3 phases cannot be stabilized unless the growth temperature is reduced to 450 K. As a result, a small amount of β-In_2Se_3 phases are observed to survive the $\beta \rightarrow \gamma$ process (co-existence of both γ- and β-In_2Se_3 phases in an In_2Se_3 sample grown at 430 K are detected by XRD as shown in the lower part of Fig. 2(a)). Further reduction of the substrate temperature to lower than 450 K leads to PC film consisting of α-, β-, and γ-In_2Se_3 phases. Therefore, the minimum temperature to achieve pure-phased γ-In_2Se_3 film on mica is determined to ~ 450 K, which is strikingly far lower than the minimum phase equilibrium temperature of bulk γ-In_2Se_3 (~ 623 K).

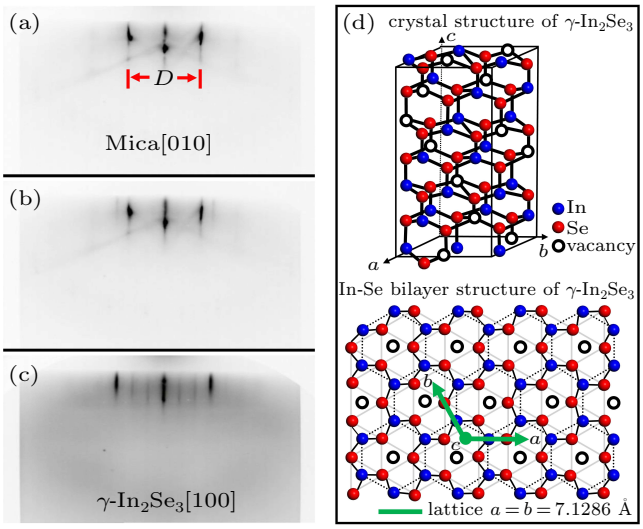


Fig. 1. RHEED patterns taken during the growth of an In_2Se_3 film. The patterns are observed in the [0 1 0] azimuth of mica substrate; (a) the mica substrate, (b) the nucleation of β-In_2Se_3 buffer layer at In nominal coverage of ~ 2 MLs, and (c) γ-In_2Se_3 film achieved after $\beta \rightarrow \gamma$ process. (d) Ball-stick illustrations of defect-wurtzite crystal structure and top In–Se bilayer structure of γ-In_2Se_3. The hexagonal Se- and honeycombed In-sublattices in the close-packed plane of γ-In_2Se_3 are indicated by solid and dotted lines, respectively.

As film thickness further increases for a few more nanometers, the streaky $\sqrt{3} \times \sqrt{3}$ RHEED pattern of γ-In_2Se_3 becomes sharper and brighter, then remains unchanged without degradation during the successive epitaxial growth, reflecting superior crystallinity and surface morphology of the obtained γ-In_2Se_3 film. Likewise, the coherent epitaxial relationship of In_2Se_3(0 0 1)[1 0 0]//mica(0 0 1)[0 1 0] can also be determined. In some cases of covalent compound growth on

layered substrates, such as ZnSe-on-Bi_2Se_3, we note that the weak chemical bonding between the absorbates and substrate often leads to the three-dimensional growth mode of these heteroepitaxial systems.[24] For the In_2Se_3-on-mica case in this study, the initial two-dimensional β-In_2Se_3 buffer layer of the layered structure is above all favored in a so-called van der Waals epitaxy growth mechanism,[25–27] since a fast lattice relaxation process between the β-In_2Se_3 and mica is observed by the RHEED. The subsequent $\beta \rightarrow \gamma$ process should also be of minimized strain, due to the quite small lattice mismatch between β-In_2Se_3 (~ 4 Å) and γ-In_2Se_3 (noting that the hexagonal Se sublattice constant in c-plane of γ-In_2Se_3 is ~ 4.1 Å), which facilitates the smooth growth fronts formation of the covalent γ-In_2Se_3 on mica. It should be noted that the mica surface is more chemically inert than that of GaAs. Hence, it is reasonable to expect that the van der Waals epitaxy mode of In_2Se_3 is energetically more favorable on mica than on GaAs, which could also be responsible for the realization of In_2Se_3 epitaxy at lower growth temperature on mica than on GaAs.

The upper part of Fig. 2(a) displays the XRD spectrum of a 60 nm thick film obtained at 480 K showing peaks at 2θ angles of 27.6° and 56.7° corresponding to (0 0 6) and (0 0 12) planes of γ-In_2Se_3, respectively. The peaks other than (0 0 6) and (0 0 12) planes belong to the mica substrate. No impurity peaks are observed, confirming the phase purity of the as-grown γ-In_2Se_3 film. As a comparison, one can find (0 0 3) and (0 0 6) peaks of β-In_2Se_3, locating at 2θ angles of 9.4° and 18.8°, in addition to the peaks of mica and γ-In_2Se_3, in the XRD curve of an In_2Se_3 film grown at 430 K (lower part of Fig. 2(a)), which witnesses the preserving of some β-In_2Se_3 phases across the $\beta \rightarrow \gamma$ process at the low growth temperature. Now we focus on the pure-phased γ-In_2Se_3 samples. x-ray rocking curve (ω-scan) of the (0 0 6) plane of γ-In_2Se_3 gives a full width at half maxima (FWHM) value of 0.5522°, which is a rather large value compared to that of the mica substrate ($< 0.1°$), depicting the slightly tilting of the γ-In_2Se_3 film around the coherent [0 0 1] axis. XRD Φ-Scans of the mica (2 0 2) and γ-In_2Se_3 (1 1 6) are depicted in Fig. 2(b). The mica and the film display tri-fold and six-fold symmetric reflection peaks, respectively, reflecting their monoclinic and hexagonal symmetries. The Φ angle between mica (2 0 2) and γ-In_2Se_3 (1 1 6) peaks is 30°, verifying the In_2Se_3(0 0 1)[1 0 0]//mica(0 0 1)[0 1 0] epitaxial relation as suggested by RHEED observations. Raman spectroscopies at 532 nm laser illumination are exhibited in Fig. 2(c). All the resolved phonon structures in the Raman spectrum of γ-In_2Se_3 on mica sample can be precisely identified to γ-In_2Se_3,[28–30] except the 102 cm^{-1}, 196 cm^{-1}, 276 cm^{-1}, 315 cm^{-1}, and 372 cm^{-1} peaks, which are from the mica substrate. The Gaussian fitted FWHM value of the most prominent peak at 151 cm^{-1} (the zone center vibration mode of γ-In_2Se_3) is 0.87559 cm^{-1} (Fig. 2(d)), which is smaller than that of PC γ-In_2Se_3 ever reported, thus manifests the promoted crystallinity of the obtained SC γ-In_2Se_3 film.

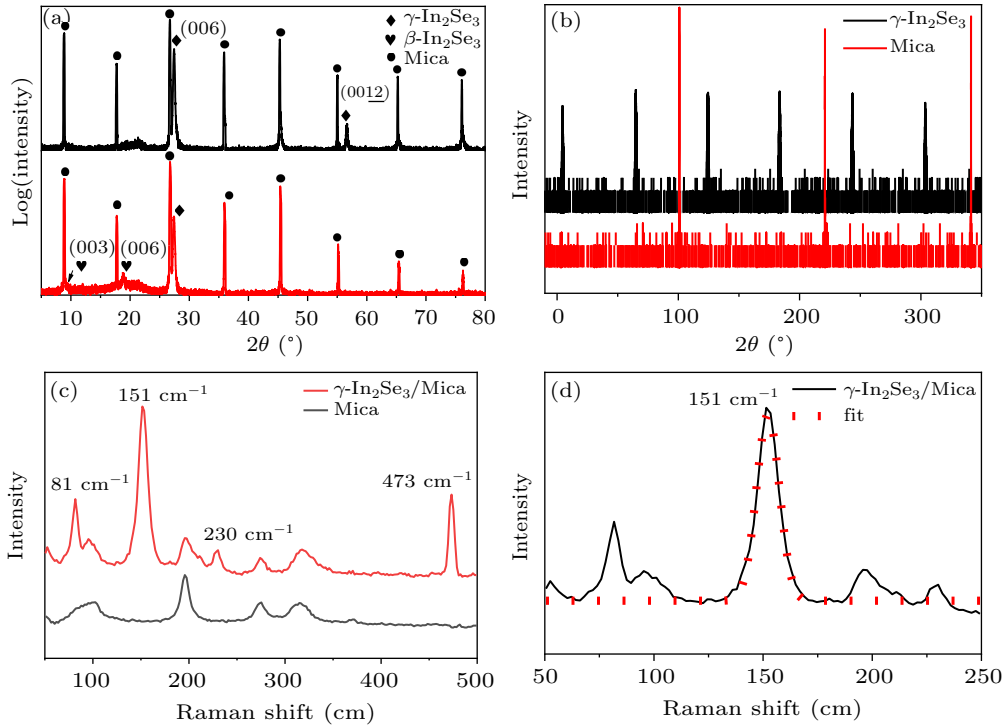


Fig. 2. (a) XRD out-of-plane 2θ–ω scans of two In_2Se_3 films grown on mica, respectively. The upper curve is from a pure γ-In_2Se_3 sample obtained at 480 K. While the lower curve is from an In_2Se_3 sample prepared at 430 K. The thickness of both films is 60 nm. (Noting that the Miller index (0 0 12) is written as (00$\underline{12}$) here for saving space) (b) XRD in-plane Φ scans of the γ-In_2Se_3 sample obtained at a higher temperature of (a). (c) illustrates Raman spectra of the same sample of (b). The lower Raman curve is from a pure mica substrate. (d) The Gaussian fitting of the 151 cm^{-1} Raman peak of (c).

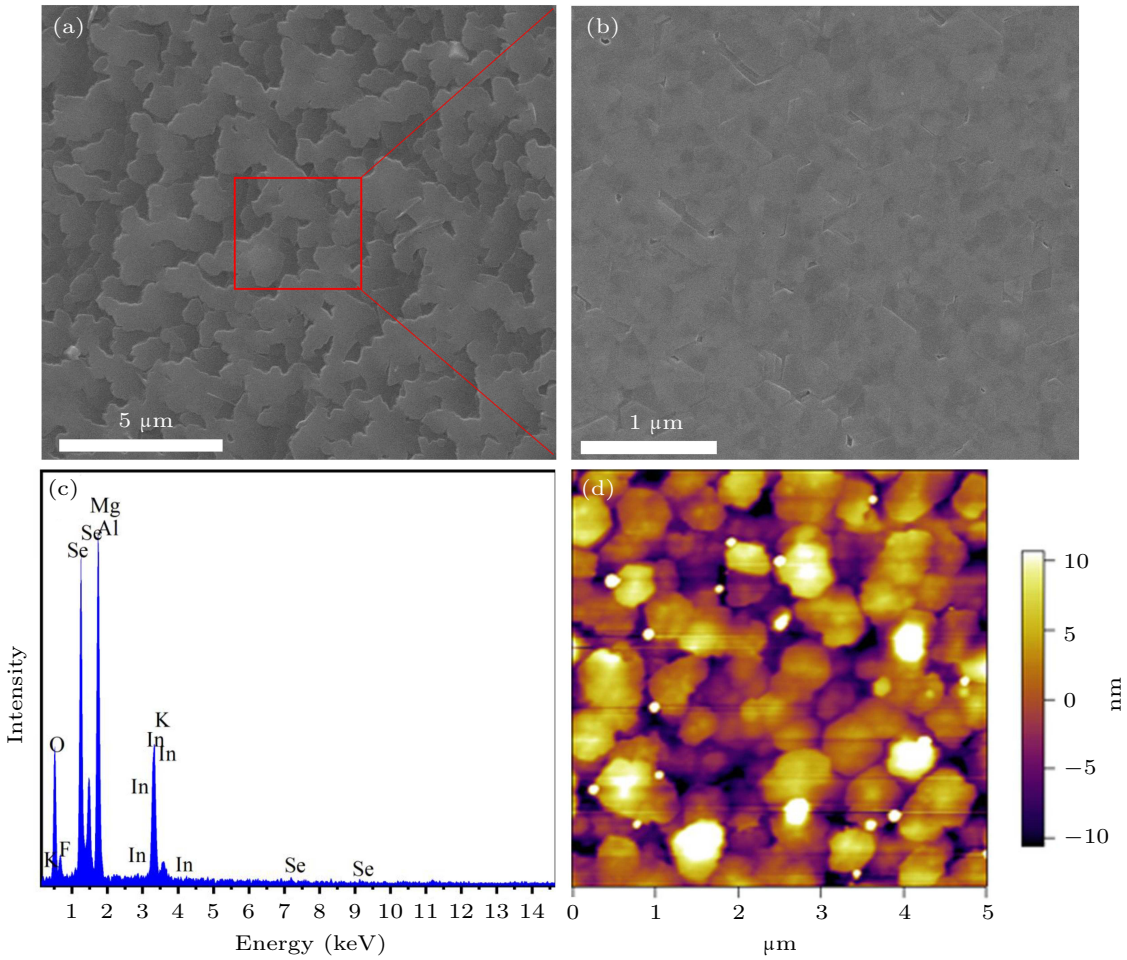


Fig. 3. (a) Large-size SEM image of a γ-In_2Se_3 thin film deposited at the substrate temperature of 480 K and with a thickness of 60 nm. (b) A zoom-in SEM image exhibiting the stacked nanoflakes surface morphologies of the same sample. (c) EDS spectrum of the γ-In_2Se_3 film on mica. (d) An AFM image from the same γ-In_2Se_3 sample in (a).

Figures 3(a) and 3(b) display large-size and zoom-in SEM images of γ-In_2Se_3 thin film, respectively, exhibiting deposition of microflakes of micrometer dimension and smooth surfaces stacked on one another. The AFM measurements of the same sample further reveal the surfaces of microflakes displayed in Figs. 3(a) and 3(b) are slightly rough (RMS roughness $\sim$ 3 nm) and decorated with small nanocrystals (Fig. 3(d)). Such surface morphologies may reflect an out-of-plane mosaic structure of the epifilm since there is lattice tilting in [0 0 1] epitaxial orientation as revealed by XRD. EDS composition study of the as-grown γ-In_2Se_3 thin film is shown in Fig. 3(c), which demonstrates the presence of In and Se.

Figure 4(a) presents the 532 nm laser-illuminated PL spectrum of the γ-In_2Se_3 film with PL peak positioned at 1.94 eV, which is in good agreement with the previous literature.[31–33] The existence of PL spectrum depicts the production of photo-induced charge carriers, which is a vital property of semiconductor material for its application in optoelectronic/photovoltaic devices. As a proof-of-concept, a simple device is fabricated by manually pasting two In-Ga eutectic alloy electrodes to the two sides of the short edges of a 200 nm thick γ-In_2Se_3 epifilm (with plane geometry of 10 mm $\times$ 4.5 mm), respectively, to inspect the optoelectronic response under the illumination from a standard sun solar simulator (AM 1.5 G, 100 mW/cm^2). The calculated resistivity from the dark I–V curve of the SC γ-In_2Se_3 epifilm is $\sim 6 \times 10^4$ Ω·cm, which is almost 3 to 4 orders of magnitude smaller than that of PC γ-In_2Se_3 films,[34,35] on the other hand, implying enhanced carrier mobility and/or increased carrier density of the SC film. Under the illumination of light, the current in the 200 nm thick SC γ-In_2Se_3 film shows nearly ten times higher value compared to its value in the dark, suggesting improved photoresponse as compared to that of PC γ-In_2Se_3 nanocrystals achieved by chemical routes.[36] Anyway, we also note that a much higher current ratio of $\sim$ 50 under light and dark conditions is reported in sputtered thick PC γ-In_2Se_3 film.[37] Because there's commonly higher defect density in PC materials than in their SC counterparts, one cannot simply ascribe the degraded photoresponse in SC γ-In_2Se_3 films compared with its PC counterparts to carriers trapping effects brought about by bulk defects. We thus speculate the photogenerated carrier kinetics in our SC γ-In_2Se_3 thin films would be subjected to some surface trapping processes since the film thicknesses of the samples in our experiments are thin

enough (i.e., no more than two hundred nanometers) to give a large surface area-to-volume ratio. In another experiment carried out on a thinner SC γ-In_2Se_3 film (100 nm), we observe little photoresponse under the same illumination condition applied to the thicker sample, which in a way verifies surface states' contribution to the photoelectric transport increases rapidly as thickness decreases. Therefore, prior to optoelectronic device applications, it should be necessary to use thick films and/or effectively passivate the surface states of SC γ-In_2Se_3. On the other side, the surface-sensitive optoelectronic characteristics might be favorable in photocatalytic applications of thin SC γ-In_2Se_3 films.[38]

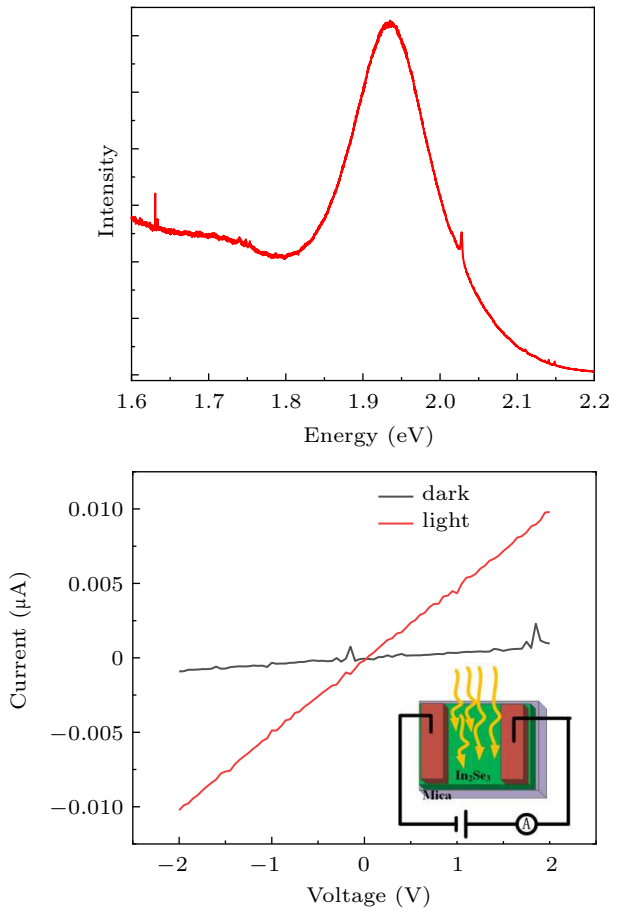


Fig. 4. (a) PL spectra of a 200 nm thick γ-In_2Se_3 thin film. (b) Current-voltage (I–V) characteristics of the same film in the presence and absence of light (inset shows a schematic diagram of the device configuration for the measurements).

4. Conclusions

In summary, single-crystalline γ-In_2Se_3 thin films are epitaxially grown on mica by molecular beam epitaxy at low temperature. An ultrathin β-In_2Se_3 van der Waals type buffer layer is confirmed to form through a self-organization growth during initial deposition, which facilitates subsequent monolithic epitaxy of metastable γ-In_2Se_3. The achieved single-crystalline γ-In_2Se_3 thin films exhibit strong room-temperature photoluminescence and moderate optoelectronic response, thus are suitable for further device development. The method presented in this paper would lay the foundation for future epitaxial integration of γ-In_2Se_3 on various van der Waals type materials or microelectronic circuits at device-process compatible growth temperature conditions.

Acknowledgement

We thank Dr. Jing Ni and Mr. Dechao Xu for their help in preparing mica substrates.

References

[1] Emziane M, Marsillac S and Bernède J C 2000 *Mater. Chem. Phys.* **62** 84
[2] Balakrishnan N, Staddon C R, Smith E F, Stec J, Gay D, Mudd G W, Makarovsky O, Kudrynskyi Z R, Kovalyuk Z D, Eaves L, Patanè A and Beton P H 2016 *2D Mater.* **3** 025030
[3] Wu C Y, Kang J W, Wang B, Zhu H N, Li Z J, Chen S R, Wang L, Yang W H, Xie C and Luo L B 2019 *J. Mater. Chem. C* **7** 11532
[4] Ohtsuka T, Nakanishi K, Okamoto T, Yamada A, Konagai M and Jahn U 2001 *Jpn. J. Appl. Phys.* **40** 509
[5] Jasinski J, Swider W, Washburn J, Liliental-Weber Z, Chaiken A, Nauka K, Gibson G A and Yang C C 2002 *Appl. Phys. Lett.* **81** 4356
[6] Lee H, Kang D H and Tran L 2005 *Mater. Sci. Eng. B* **119** 196
[7] Hsiao Y J, Lu C H, Ji L W, Meen T H, Chen Y L and Chi H P 2014 *Nanoscale Res. Lett.* **9** 32
[8] Shi H, Li M, Shaygan Nia A, Wang M, Park S, Zhang Z, Lohe M R, Yang S and Feng X 2020 *Adv. Mater.* **32** 1907244
[9] Julien C, Hatzikraniotis E, Chevy A and Kambas K 1985 *Mater. Res. Bull.* **20** 287
[10] Cui J, Peng H, Song Z, Du Z, Chao Y and Chen G 2017 *Chem. Mat.* **29** 7467
[11] Balakrishnan N, Steer E D, Smith E F, Kudrynskyi Z R, Kovalyuk Z D, Eaves L, Patanè A and Beton P H 2018 *2D Mater.* **5** 035026
[12] Poh S M, Tan S J R, Wang H, Song P, Abidi I H, Zhao X, Dan J, Chen J, Luo Z, Pennycook S J, Castro Neto A H and Loh K P 2018 *Nano Lett.* **18** 6340
[13] Ye J, Yoshida T, Nakamura Y and Nitton O 1995 *Appl. Phys. Lett.* **67** 3066
[14] Ye J, Soeda S, Nakamura Y and Nittono O 1998 *Jpn. J. Appl. Phys.* **37** 4264
[15] Yan Y, Li S, Ji Y, Liu L, Yan C, Zhang Y, Yu Z and Zhao Y 2013 *Mater. Lett.* **109** 291
[16] Amory C, Bernède J C and Marsillac S 2003 *J. Appl. Phys.* **94** 6945
[17] Wei D, Lin Z, Cui Z, Su S, Zhang D, Cao M and Hu C 2013 *Chem. Commun.* **49** 9609
[18] Chang K J, Lahn S M and Chang J Y 2006 *Appl. Phys. Lett.* **89** 182118
[19] Lyu D Y, Lin T Y, Lin J H, Tseng S C, Hwang J S, Chiang H P, Chiang C C and Lan S M 2007 *Sol. Energy Mater. Sol. Cells* **91** 888
[20] Ohtsuka T, Nakanishi K, Okamoto T, Yamada A, Konagai M and Jahn U 2001 *Jpn. J. Appl. Phys.* **40** 509
[21] Li H, Ren W, Wang G, Gao L, Peng R, Li H, Zhang P, Shafa M, Tong X, Luo S, Zhou Z, Ji H, Wu J, Niu X and Wang Z 2016 *J. Phys. D: Appl. Phys.* **49** 145108
[22] Ren W, Li H, Gao L, Li Y, Zhang Z, Long C, Ji H, Niu X, Lin Y and Wang Z 2017 *Nano Res.* **10** 247
[23] Shen Y, Yin X, Xu C, He J, Li J, Li H, Zhu X and Niu X 2020 *Chin. Phys. B* **29** 056402
[24] Li H D, Wang Z Y, Guo X, Wong T L, Wang N and Xie M H 2011 *Appl. Phys. Lett.* **98** 043104
[25] Atsushi K 1992 *Thin Solid Films* **216** 72
[26] Li H D, Wang Z Y, Kan X, Guo X, He H T, Wang Z, Wang J N, Wong T L, Wang N and Xie M H 2010 *New J. Phys.* **12** 103038
[27] Li H, Gao L, Li H, Wang G, Wu J, Zhou Z and Wang Z 2013 *Appl. Phys. Lett.* **102** 074106
[28] Marsillac S, CombotMarie A M, Bernede J C and Conan A 1996 *Thin Solid Films* **288** 14
[29] Weszka J, Daniel P, Burian A, Burian A M and Nguyen A T 2000 *J. Non-Cryst. Solids* **265** 98

[30] Lyu D Y, Lin T Y, Chang T W, Lan S M, Yang T N, Chiang C C, Chen C L and Chiang H P 2010 *J. Alloy. Compd.* **499** 104
[31] Ohtsuka T, Okamoto T, Yamada A and Konagai M 2000 *J. Lumines.* **87** 293
[32] Yang M D, Hu C H, Shen J L, Lan S M, Huang P J, Chi G C, Chen K H, Chen L C and Lin T Y 2008 *Nanoscale Res. Lett.* **3** 427
[33] Chang K J, Lahn S M, Xie Z J, Chang J Y, Uen W Y, Lu T U, Lin J H and Lin T Y 2007 *J. Crys. Growth* **306** 283
[34] Chaiken A, Nauka K, Gibson G A, Lee H, Yang C C, Wu J, Ager J W, Yu K M and Walukiewicz W 2003 *J. Appl. Phys.* **94** 2390
[35] Okamoto T, Nakada Y, Aoki T, Takaba Y, Yamada A and Konagai M 2006 *Phys. Stat. Sol. (c)* **3** 2796
[36] Ho C H 2014 *Sci. Rep.* **4** 4764
[37] Yan Y, Li S, Yu Z, Liu L, Yan C P, Zhang Y and Zhao Y 2014 *Opt. Mater.* **38** 217
[38] Yang S, Xu C Y, Yang L, Hu S P and Zhen L 2016 *RSC Adv.* **6** 106671